JOURNAL OF GEOPHYSICAL RESEARCH, VOL. 105, NO. D12, PAGES 15,231–15,245, JUNE 27, 2000

A near-infrared optimized DOAS method for the fast global retrieval of atmospheric CH_4, CO, CO_2, H_2O, and N_2O total column amounts from SCIAMACHY Envisat-1 nadir radiances

Michael Buchwitz, Vladimir V. Rozanov, and John P. Burrows

Institut für Fernerkundung, Universität Bremen, Bremen, Germany

Abstract. A new method for the fast and accurate retrieval of atmospheric trace gas total column amounts from near-infrared nadir radiances, to be measured by the scanning imaging absorption spectrometer for atmospheric chartography (SCIAMACHY) spectrometer on board the European Space Agency Envisat-1 satellite, has been investigated. It can be characterized as a weighting function modified differential optical absorption spectroscopy approach (WFM-DOAS). The reference spectra of the linear fit include the trace gas total column weighting functions, a weighting function for a temperature profile shift, and a low-order polynomial. Systematic errors due to uncertainties in atmospheric and surface parameters which cannot be retrieved, such as the trace gas vertical profile shapes, pressure and temperature profiles, aerosols, and the surface reflectivity, are quantified. The total column precisions of all trace gases to be retrieved from the SCIAMACHY near-infrared channels 7 (1940-2040 nm) and 8 (2265-2385 nm) have been estimated to be better than 1% for H_2O, CO_2, and CH_4, and better than 10% for N_2O and CO. The potential of SCIAMACHY to measure regional CO_2 and CH_4 emission fluxes has been investigated. Both are important greenhouse gases to be monitored and reduced according to the Kyoto Protocol of the U.N. Framework Convention on Climate Change.

1. Introduction

The scanning imaging absorption spectrometer for atmospheric chartography (SCIAMACHY) instrument [*Burrows et al.*, 1995; *Bovensmann et al.*, 1999] is a multichannel diode array satellite spectrometer covering the spectral range 240-2385 nm with moderate resolution (0.2-1.6 nm) and will observe the Earth's atmosphere in nadir and limb, and solar and lunar occultation viewing geometries. SCIAMACHY is part of the atmospheric sciences payload of the European Space Agency (ESA) Envisat-1 satellite due for launch in mid 2001. This study presents the first detailed investigation concerning CH_4, CO, CO_2, H_2O, and N_2O total column retrieval using the near-infrared (NIR) nadir measurements of SCIAMACHY. All these gases play a significant role in climate change: directly, with the exception of CO, as they are important greenhouse gases [*Intergovernmental Panel on Climate Change (IPCC)*, 1995], or indirectly, as for CO, which influences the tropospheric OH and thereby the CH_4 concentration [*Daniel and Solomon*, 1998]. In addition, these species and their reactions are important in determining the ozone concentration in the troposphere and the stratosphere [see, e.g., *Crutzen et al.*, 1999; *Solomon*, 1999, and references therein].

SCIAMACHY has eight spectral channels, with 1024 individual detector diodes per channel, observing simultaneously the regions 240-1750 nm (channels 1-6), 1940-2040 nm (channel 7), and 2260-2385 nm (channel 8). The absolute radiometric accuracy required for SCIAMACHY is 3-4% for the Sun-normalized radiance measurements, that is, for the ratio of earthshine radiance and extraterrestrial solar irradiance. The required relative accuracy within one channel is 0.02% (excluding noise). Details about atmospheric constituents to be measured using the channels 1-6 or the limb and occultation modes of SCIAMACHY, not discussed in this study, are given by *Bovensmann et al.* [1999].

This study focuses on the retrieval of atmospheric trace gas total column amounts from the NIR nadir Sun-normalized radiance measurements using channel 7 (1940-2040 nm, spectral resolution 0.21 nm as characterized by the full width at half maximum (FWHM) of the bell-shaped (approximately Gaussian) instrument slit function) and channel 8 (2260-2385 nm, 0.24 nm FWHM). The spectral region covered by channel 7 is dominated by strong CO_2 and H_2O absorption,

Paper number 2000JD900191.
0148-0227/00/1999JD900191$09.00

the channel 8 region by strong absorption due to CH_4 and H_2O and relatively weak absorption bands of CO and N_2O. The approximate spectral sampling intervals (wavelength grid), or equivalently, the spectral interval covered by each of the (consecutively arranged) 1024 detector diodes per channel, is about half the spectral resolution FWHM of a given channel. In nadir mode, SCIAMACHY is across-track scanning ± 30° around the nadir direction (for the nominal swath width) resulting in four ground pixels of 30×240 km^2 each (along track times across track) for an integration time of 1 s.

Trace gas total column amounts of, for example, ozone, NO_2, BrO, or SO_2, can be derived from scattered and reflected ultraviolet and visible solar radiation detected from space, using the "standard" differential optical absorption spectroscopy (DOAS) algorithm, as demonstrated by the global ozone monitoring experiment (GOME) instrument [*Burrows et al.*, 1999; *Eisinger and Burrows*, 1998; *Richter et al.*, 1998, and references therein]. GOME on the ERS-2 satellite is a small-scale version of SCIAMACHY restricted to nadir measurements in the 240-790 nm spectral region. The first four channels of GOME and SCIAMACHY are nearly identical. GOME has been successfully providing data since April 1995. The standard GOME-DOAS algorithm is in principle identical with the DOAS algorithm widely used by the atmospheric science community for the retrieval of vertical column amounts from ground-based zenith sky measurements of scattered radiation in the UV-visible region (see references given by *Bovensmann et al.* [1999]).

The GOME-DOAS algorithm retrieves the trace gas total column (also called vertical column density (VCD)) in a two-step approach. In a first step, trace gas slant column densities (SCD) are determined by linear least squares fitting a combination of trace gas absorption cross sections, a low-order polynomial, and a Ring reference spectrum (to account for inelastic Raman scattering), to the measured optical depth, defined as the negative logarithm of the ratio of earthshine radiance and solar irradiance. The SCD of a given trace gas is converted in a second step to the desired VCD by dividing the SCD with an appropriate air mass factor (AMF), obtained by radiative transfer simulation.

This standard DOAS algorithm is based on several assumptions, mainly related to the pressure and temperature, and therefore altitude, and wavelength dependence of the trace gas absorption cross section. The DOAS algorithm applied to measurements of scattered light also requires that the trace gas absorption is weak, as standard DOAS is based on the assumption that the logarithm of the radiance depends linearly on the trace gas vertical column amount (Beer-Lambert law). Furthermore, the Beer-Lambert law is strictly valid only for monochromatic radiance measurements, an assumption not valid for radiation that strongly depends on wavelength within spectral intervals as defined by the instrument resolution. Due to the much stronger dependence of the trace gas absorption cross sections in the near-infrared spectral region on pressure, temperature, and wavelength, and because the absorption is generally quite strong, the standard DOAS algorithm cannot directly be applied to NIR measurements (or to water vapor retrieval in the visible). One reason is simply that the standard DOAS algorithm requires an absorption cross section reference spectrum for each trace gas that absorbs in a given spectral fitting window. If, however, the absorption cross section strongly depends on altitude, the selection of an absorption cross section spectrum valid for one altitude only may introduce large total column errors.

A significant modification of the standard DOAS algorithm, called weighting function modified (WFM) DOAS, is presented in this paper, appropriate also for the NIR spectral region. The WFM-DOAS algorithm is based on approximating the logarithm of the measured Sun-normalized radiance by a corresponding linearized model quantity (i.e., using the mean radiance and its derivatives calculated for a given model atmosphere) plus a low-order polynomial. The main difference between both algorithms is that the trace gas absorption cross section reference spectra used by standard DOAS are replaced by trace gas total column weighting functions, that is, by spectra representing the relative radiance change due to a vertical profile change (applying an altitude-independent scaling factor to the entire profile). The WFM-DOAS fit parameters are the desired vertical columns (more precisely: the column difference with respect to the known column of a model atmosphere). This eliminates the need for an air mass factor conversion. It can be shown that the standard DOAS equation (based on cross section reference spectra) can be derived from the WFM-DOAS equation (based on weighting function reference spectra; see section 3), if (1) the trace gas absorption cross sections are altitude independent, and (2) the atmosphere is optically thin (see *Rozanov et al.* [1998], discussing standard DOAS AMFs and AMFs derived using weighting functions). As the WFM-DOAS equation is a generalization of the standard DOAS equation, the WFM-DOAS algorithm can also be applied to the UV-visible spectral region as standard DOAS. Apart from WFM-DOAS, several other modifications have been proposed to improve the standard DOAS algorithm focusing on the UV-visible spectral range [*Diebel et al.*, 1995; *Richter*, 1997; *Burrows et al.*, 1999; *Noël et al.*, 1999].

The structure of this paper is as follows: section 2 is introducing the radiative transfer model used for this study, including a discussion of the radiative transfer aspects relevant for the spectral region around 2 μm. In section 3 the WFM-DOAS algorithm is presented. The algorithm is investigated in section 4 using simulated SCIAMACHY nadir measurements around 2.3 μm. Section 5 estimates the trace gas total column retrieval precisions taking into account the measurement noise. The potential of SCIAMACHY to measure re-

gional greenhouse gas emission fluxes is discussed in section 6.

2. Radiative Transfer in the 2 μm Spectral Region

The radiative transfer model SCIATRAN used for this study provides numerical solutions of the monochromatic scalar radiative transfer (RT) equation for a plane-parallel vertically inhomogeneous atmosphere using the finite difference method [*Barkstrom*, 1976], taking into account multiple scattering. The sphericity of the Earth is considered by using a pseudospherical approach, that is, the solar source function (the number of solar photons reaching a given altitude before being scattered for the first time) is evaluated taking the sphericity of the Earth fully into account, including refraction. The numerical solution of the RT equation, as determined by SCIATRAN, is the Sun-normalized radiance (here the radiance for a constant solar flux of π), in this study also called intensity.

SCIATRAN is an extension of the GOMETRAN RT model [*Rozanov et al.*, 1997], in particular with respect to molecular line absorption due to CH_4, CO, CO_2, H_2O, N_2O, and O_2 in the 440-2400 nm spectral region. For this purpose, a fast correlated-k distribution scheme has been developed [*Buchwitz et al.*, 1998, 1999, 2000], taking into account the instrument resolution. This scheme is used for this study. The correlated-k coefficients (representative absorption cross sections for finite spectral intervals) were generated using the HITRAN 96 database of spectroscopic line parameters [*Rothman et al.*, 1998]. Alternatively, a line-by-line scheme has also been implemented, mainly for reference purposes. The correlated-k and the line-by-line radiances agree to within better than 1-2% after convolution with the SCIAMACHY slit function. This holds for the entire spectral region covered by SCIAMACHY. In this study, retrieval errors due to uncertainties in spectroscopic parameters are not considered. For a discussion of the quality of the HITRAN 96 data in the spectral region covered by channel 8, see *Edwards et al.* [1999].

In addition to molecular line absorption, absorption due to ozone, NO_2, BrO, and other trace gases absorbing in the ultraviolet and visible spectral regions, is implemented in SCIATRAN, as well as Rayleigh scattering by air molecules. Parameterization schemes for scattering and absorption by clouds [*Kurosu et al.*, 1997] and aerosols [*Hoogen*, 1995; *Kauss*, 1998] (and the MODTRAN aerosol model based on *Shettle and Fenn* [1979]) are implemented for the 240-2400 nm spectral region. For this study only the MODTRAN [*Kneizys et al.*, 1996] aerosol model has been used. Rotational Raman scattering by air molecules ("Ring effect") can be considered [*Vountas et al.*, 1998]. Thermal (Planck) emission of the atmosphere and the surface has also been implemented recently. The Earth's surface is modeled for this study as a wavelength-independent Lambertian reflector.

SCIATRAN enables derivatives of the top-of-atmosphere radiance (i.e., weighting functions) with respect to many atmospheric parameters and albedo changes to be determined quasi-analytically [*Rozanov et al.*, 1998]. These derivatives of the radiance in addition to the radiance itself are needed for the retrieval algorithm presented in this study. This quasi-analytical weighting function scheme, which provides altitude-resolved weighting functions, enables time-consuming numerical perturbation methods, which are usually applied to determine the weighting functions, to be entirely avoided. This scheme is based on solving the linearized RT equation, derived by introducing analytical variations for all relevant atmospheric parameters in the (nonlinearized) RT equation. These parameters are, for example, the concentration of all trace gases at all altitude levels. Solving the linearized RT equation, for the changes of the radiance due to changes in the atmospheric parameters, only requires a negligible amount of additional computational effort. This is due to the fact that the same inverted matrix needed for the radiance calculation is also required to solve the linearized RT equation, that is, no additional (time consuming) matrix inversion needs to be performed.

All results presented in this study are based on full multiple scattering radiative transfer simulations. Although scattering in the 2 μm spectral region is less important in comparison with the UV-visible region, it has been shown that scattering, even multiple scattering, cannot be neglected [*Buchwitz et al.*, 1999]. Typically, 10% of the photons observed in nadir viewing geometry from space have been scattered more than once in the spectral region 2260-2385 nm corresponding to SCIAMACHY channel 8 [*Buchwitz et al.*, 1999]. In this spectral region the ratio of two radiance spectra calculated assuming single scattering and full multiple scattering show, in addition to the 10% offset, differential structures which are correlated with strong H_2O and CH_4 absorption features. The amplitude of these structures is of the order of a few percent, that is, comparable in magnitude with typical overlapping CO and N_2O absorption structures.

The filling-in of Fraunhofer lines and atmospheric absorption structures in scattered light due to inelastic rotational Raman scattering (Ring effect) usually needs to be considered for DOAS total column retrieval in the UV-visible spectral region [see, e.g., *Vountas et al.*, 1998]. SCIATRAN simulations in the 2360 nm spectral region show that the effect of rotational Raman scattering on the radiance is generally less than 0.01% for SCIAMACHY nadir measurements. The Ring effect may reach 0.1% in spectral regions showing very strong absorption features. The Ring effect can therefore be neglected for SCIAMACHY channel 8 retrieval.

In the spectral region covered by SCIAMACHY (240-

2385 nm) the majority of the photons detected from space in nadir viewing geometry are solar photons reflected from the surface or scattered in the atmosphere. SCIATRAN radiative transfer simulations show that below 2360 nm the fraction of photons generated by thermal emission is generally well below 1% at SCIAMACHY resolution. In between 2360-2385 nm (end of channel 8), however, the radiance levels are very low due to strong H_2O and CH_4 absorption structures, and the effect of thermal emission on the top-of-atmosphere radiance may reach 3%. For the retrieval study presented here, thermal emission has been neglected. The corresponding retrieval error is assumed to be negligible but has not been quantified yet.

As SCIATRAN solves the scalar RT equation and not the full vector RT equation based on the Stokes vector formalism, polarization has been neglected for this study. The scalar RT equation accurately accounts for single scattering but introduces intensity errors for higher orders of scattering [e.g., *Stammes*, 1994]. Therefore the error introduced by neglecting polarization increases with increasing multiple scattering. Multiple scattering decreases with increasing wavelength and increasing atmospheric absorption. For SCIAMACHY nadir observations, the largest error introduced by neglecting polarization should appear in the spectral region 300-350 nm (below 300 nm the strong ozone absorption significantly reduces the fraction of multiply scattered light). In this region the error on the radiance introduced by neglecting polarization can reach about 5% [*Stammes*, 1994]. This error is assumed to be much smaller in the NIR spectral region investigated in this study.

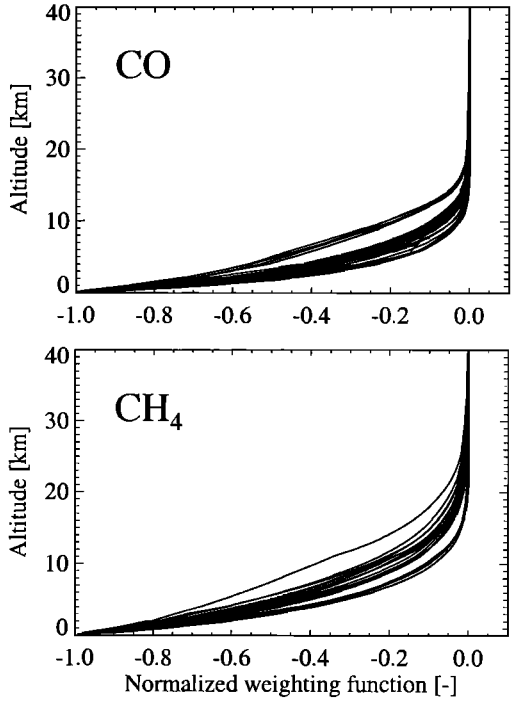

Figure 1. Typical SCIAMACHY CO and CH_4 number density weighting functions for nadir observations. Each curve corresponds to a different detector pixel center wavelength of SCIAMACHY channel 8. They show, for a given altitude, the radiance change corresponding to a constant, that is, altitude-independent, relative concentration change at that altitude. Each weighting function has been normalized to its maximum value. Scenario: U.S. Standard Atmosphere, solar zenith angle 40°, and albedo 0.2.

3. Weighting Function Modified DOAS Method

In this section a fast and accurate approach for the retrieval of trace gas total column amounts from near-infrared nadir radiance measurements is presented. The error on the retrieved vertical columns due to a priori assumptions concerning trace gas vertical profile shapes, interfering trace gases, pressure and temperature profiles, aerosol scattering and extinction, and surface reflectivity is quantified. This study focuses on ground pixels classified as cloud free. The fraction of a SCIAMACHY ground pixel covered by clouds can be determined, as shown by GOME, by several means, for example, by analyzing the radiances inside and outside the oxygen A-band region around 760 nm (channel 4) and by using the subpixel information provided by the polarization measurement devices [e.g., *Kurosu et al.*, 1998; *Burrows et al.*, 1999; *Bovensmann et al.*, 1999].

Before focusing on trace gas total column retrieval, it is interesting to investigate first if height-resolved information can be obtained from the nadir observations. The retrieval of vertical profiles of ozone [*Hoogen et al.*, 1999] or temperature [*Rodgers*, 1976] from satellite nadir radiance measurements generally requires that the corresponding weighting functions peak at different altitudes for different wavelength. Here, weighting function refers to the derivative of the radiance at top of atmosphere with respect to profile changes at different altitudes.

Figure 1 shows typical altitude-resolved number density profile weighting functions for CO and CH_4 calculated with SCIATRAN for several wavelength corresponding to channel 8. Each weighting function, expressing the top of atmosphere radiance change for an altitude-independent relative concentration change (e.g., +100%) at the given altitude, peaks at the surface and decreases monotonically with increasing altitude. From the similarity of the weighting functions it can be concluded that no significant height-resolved CO and CH_4 information can be derived from the SCIAMACHY nadir measurements (for this purpose the limb and occultation measurements have to be used). However, CO and CH_4 total column information can be derived from the nadir observations as will be shown in this study. Similar remarks hold for N_2O. Total column weighting functions, expressing the radiance change for an altitude-independent relative change of the trace gas concentration profile (scaling factor), as required for

WFM-DOAS, can be obtained by vertically integrating the altitude-resolved weighting functions from the surface to the top of the atmosphere.

The weighting function modified DOAS algorithm as described in the following, is, as the standard DOAS algorithm, a linear least squares algorithm which extracts the total column information only from differential trace gas absorption features, as all (multiplicative) broadband contributions that affect the radiance are compensated by a low-order polynomial $P(\lambda)$. Therefore the retrieval is relatively insensitive to aerosols, optically thin clouds, surface reflectivity, and trace gas continuum absorption, e.g., due to H_2O. The polynomial subtraction also reduces the sensitivity for broadband residual radiometric calibration errors. However, all DOAS algorithms require an accurate spectral calibration. The spectral knowledge and stability for SCIAMACHY measurements is expected to be better than about 1/20 of a detector pixel (corresponding to 0.007 nm for channel 8). In order to correct even for small spectral misalignments between the reference and the measured spectra, a nonlinear shift-and-squeeze spectral correction algorithm is usually applied for standard DOAS retrieval. If necessary, the same procedure can also be used for WFM-DOAS. In this study, spectral calibration errors are not considered.

The logarithm of the measured intensity at wavelength λ_i, I_i^{meas}, can be approximated by a first-order Taylor expansion of an appropriate model intensity, I_i^{mod}, plus a low-order polynomial P_i:

$$\begin{aligned}\ln I_i^{\mathrm{meas}}(V^t, \mathbf{b}^t) \approx\ & \ln I_i^{\mathrm{mod}}(\bar{V}, \bar{\mathbf{b}}) \\ & + \left.\frac{\partial \ln I_i^{\mathrm{mod}}}{\partial V}\right|_{\bar{V}} \times (\hat{V} - \bar{V}) \\ & + \sum_{j=1}^{F} \left.\frac{\partial \ln I_i^{\mathrm{mod}}}{\partial b_j}\right|_{\bar{b_j}} \times (\hat{b_j} - \bar{b_j}) \\ & + P_i\,. \end{aligned} \tag{1}$$

Here V^t denotes the true vertical column of the trace gas to be retrieved, $\bar{V}$ is the corresponding assumed model column, and parameter $\hat{V}$ is the estimate of the true column to be derived from the radiance measurements, that is, the retrieved column. The retrieved column is obtained by adjusting the model intensity (entire right-hand side of (1)) to the measured intensity (left-hand side) at several spectral points λ_i simultaneously. The b_j are atmospheric and surface parameters not well known a priori and, if estimated wrong, result in differential spectral structures (i.e., fit residuals indicating a mismatch between the adjusted linear model and the measurement) that may disturb the retrieval of V^t. Candidates are the total columns of all interfering gases, as well as temperature, pressure, albedo, aerosol, and cloud parameters. In this study the temperature parameter is an altitude-independent temperature shift and the pressure parameter is a scaling factor for the entire pressure profile. The corresponding fit parameters $\hat{b_j}$ are collected in vector $\hat{\mathbf{b}}$. Vector $\mathbf{b}^t$ contains the corresponding true parameters and $\bar{\mathbf{b}}$ is the corresponding model vector (all atmospheric and surface model parameters are denoted by bars). In comparison with the standard DOAS equation, this equation differs in several aspects: (1) by introducing the model intensity spectrum, I_i^{mod}, corresponding to an assumed atmospheric state and surface reflectivity, (2) by replacing the trace gas absorption cross section reference spectra by total column weighting functions, and (3) by introducing additional terms to compensate for disturbing high-frequency spectral effects, for example, arising from atmospheric pressure and temperature effects. In line with standard DOAS the logarithm of the intensity rather than the intensity itself is modeled.

The WFM-DOAS approach requires a radiative transfer model for the accurate simulation of the intensity and its derivatives (note that $\partial \ln I/\partial x = I^{-1}\partial I/\partial x$), and the identification of atmospheric and surface parameters which might interfere with the total column information to be retrieved. In order to avoid ambiguities, the reference spectra (i.e., the derivatives of the logarithm of the intensity) need to be sufficiently spectrally uncorrelated in the selected spectral fitting window. In addition, the dependence of the logarithm of the intensity with respect to all relevant (fit) parameters must be sufficiently linear around the selected linearization point (denoted by bars).

The unknown parameters in (1), that is, $\hat{V}$, $\hat{\mathbf{b}}$, and the polynomial coefficients, can be determined by a (weighted) linear least squares minimization:

$$\|\mathbf{y} - \mathbf{A}\,\mathbf{x}\|^2 \rightarrow \text{ minimize with respect to } \mathbf{x}. \tag{2}$$

The components of vector $\mathbf{y}$ are $y_i = (\ln I_i^{\mathrm{meas}} - \ln I_i^{\mathrm{mod}})/\sigma_i$, where σ_i denotes the standard deviation of the intensity divided by the mean intensity, that is, the relative standard deviation (only relevant, if the noise level depends strongly on wavelength). Vector $\mathbf{x}$ contains the fit parameters. Component x_1 is the dimensionless total column fit parameter $(\hat{V} - \bar{V})/\bar{V}$. Components x_2 to x_{F+1} are the dimensionless parameters $(\hat{b_j} - \bar{b_j})/\bar{b_j}$. The remaining components are the polynomial coefficients. Each column of matrix $\mathbf{A}$ corresponds to one fit parameter. The first column contains the dimensionless total column weighting function, also weighted by σ_i, that is, $A_{i1} = \partial \ln I_i^{\mathrm{mod}}/\partial V|_{\bar{V}}\,\bar{V}/\sigma_i$. The following F columns are defined similarly, but for the $\hat{b_j}$. The last K columns contain the polynomial basis functions p_i^k, $k = 1, \cdots, K$, defined as $p_i^k = \lambda_i^{k-1}/\sigma_i$. The solution $\hat{\mathbf{x}}$ of (2) is

$$\hat{\mathbf{x}} = \mathbf{C_x}\,\mathbf{A}^T\,\mathbf{y}\,, \tag{3}$$

where $\mathbf{C_x} = \left(\mathbf{A^T A}\right)^{-1}$ is the solution covariance matrix and T denotes matrix transpose [see, e.g., *Press et al.*, 1992].

If the problem is not sufficiently linear to retrieve ac-

curate total columns using (1), an iterative scheme has to be used. For this purpose the linear regression has to be repeated using the results from the previous fit to update the first guess model parameters. This requires new reference spectra valid for the updated model parameters. A noniterative algorithm, however, is attractive because it is much faster. Due to the large amount of spectra to be measured by SCIAMACHY (about 1 spectrum each second), an algorithm that aims to provide global data products not only has to be accurate but also needs to be very fast. Precalculating all radiance and weighting function reference spectra permits time-consuming on-line radiative transfer simulations to be avoided. This look-up-table approach, however, requires, particularly for the planned global application, to consider the dependence of the reference spectra on several parameters which vary continuously along the orbit, such as the solar zenith angle and the viewing angles. These problems will be investigated in the following section.

4. Retrieval Studies Using Simulated Measurements

This section focuses, as an example, on CO total column retrieval from channel 8 nadir measurements in the spectral region 2310-2380 nm. As the weighting function modified DOAS approach is quite general, as explained in section 1, it also can be applied to other trace gases, spectral regions, and viewing geometries, for instance, ground-based or airborne observations.

The only near-global tropospheric CO measurements made until end of 1999 have been performed by the Measurement of Air Pollution from Satellite (MAPS) experiment from space shuttles [see *Reichle et al.*, 1990, and references therein]. MAPS detects the 4.67 μm fundamental band of CO using the gas filter correlation technique. From these measurements the average CO mixing ratio in the upper troposphere has been determined. These measurements have shown the high spatial variability of CO, and large CO sources resulting from biomass burning in the Southern Hemisphere have been identified. On December 19, 1999, the Measurement of Pollution in the Troposphere (MOPITT) instrument has been successfully launched on board the EOS Terra satellite (also known as EOS-AM1). MOPITT makes gas correlation measurements to determine the CH_4 total column (using the 2.2 μm channel) and the CO total column and profile (using its 2.3 and 4.67 μm channels) at 22×22 km^2 horizontal resolution [see *Edwards et al.*, 1999, and references therein]. The estimated total column retrieval precisions are better than 1% for CH_4 and 10% for CO [*Pan et al.*, 1998]. The spectral regions 2.2 and 2.3 μm correspond to channel 8 of SCIAMACHY.

The WFM-DOAS retrieval of CO total column amounts from simulated SCIAMACHY Sun-normalized radiance measurements in the 2310-2380 nm spectral region has been investigated to establish the CO total column error in the presence of systematic errors and to identify which additional fit parameters (b_j) need to be included.

Figure 2 shows the CO total column weighting function and the weighting functions of interfering atmospheric and surface parameters. Note that, neglecting nonlinearities (i.e., approximating $\Delta I/I$ for a given ΔV by $\partial \ln I/\partial V\, \Delta V$), these weighting functions can be transformed into transmittance spectra, simply by changing the annotation of the y axis. For example, the CO weighting function needs to be divided by 100 (to convert the percentage radiance change into an absolute radiance change). Finally, 1.0 has to be added to obtain a spectrum that can be interpreted as the radiance for an atmosphere with CO present divided by the radiance for an atmosphere without any CO present (neglecting nonlinearities, a +100% column change and a -100% column change result in the same absolute radiance change). The resulting "CO transmittance spectrum," corresponding to somewhat more than twice the vertical optical path through the atmosphere mainly due to the slant solar illumination, is about 1.0 in between the lines and on either side of the band, and about 0.96 in the center of the strongest lines. The same procedure can be applied to the H_2O and CH_4 spectra. Note that values below zero are due to nonlinearities. They would be close to zero for true transmittance spectra.

As can be seen, all weighting functions show significant spectral structures. Each trace gas can be identified by its characteristic spectral fingerprint. The weighting functions for temperature, pressure, and albedo, are, however, less characteristic and are strongly correlated with strong water vapor absorption and, to a minor extent, with methane absorption.

Test retrievals with simulated measurements have been performed for a wide range of conditions using different combinations of solar zenith angles (40°, 70°), albedo (0.05-0.2), pressure, temperature, and trace gas concentration profiles (using the six MODTRAN reference atmospheres based on *McClatchey et al.* [1972]), and aerosol scenarios. In total, more than 50 significantly different CO retrieval scenarios have been investigated. Figure 3 shows, as a typical example, the result of a WFM-DOAS fit using the total column weighting functions for CO, H_2O, and CH_4, a weighting function for a temperature shift, and a second-order polynomial (constant, linear, and quadratic terms), adjusted to simulated SCIAMACHY measurements by linear least squares minimization. The temperature weighting function has been included to consider the dependence of the trace gas absorption cross sections on the atmospheric temperature profile. The assumed model scenario comprises pressure, temperature, and CO, H_2O, and CH_4 volume mixing ratio profiles corresponding to the U.S. Standard Atmosphere [*McClatchey et al.*, 1972]. An albedo of 0.2 has been selected, a typical value for vegetation. The aerosol scenario is character-

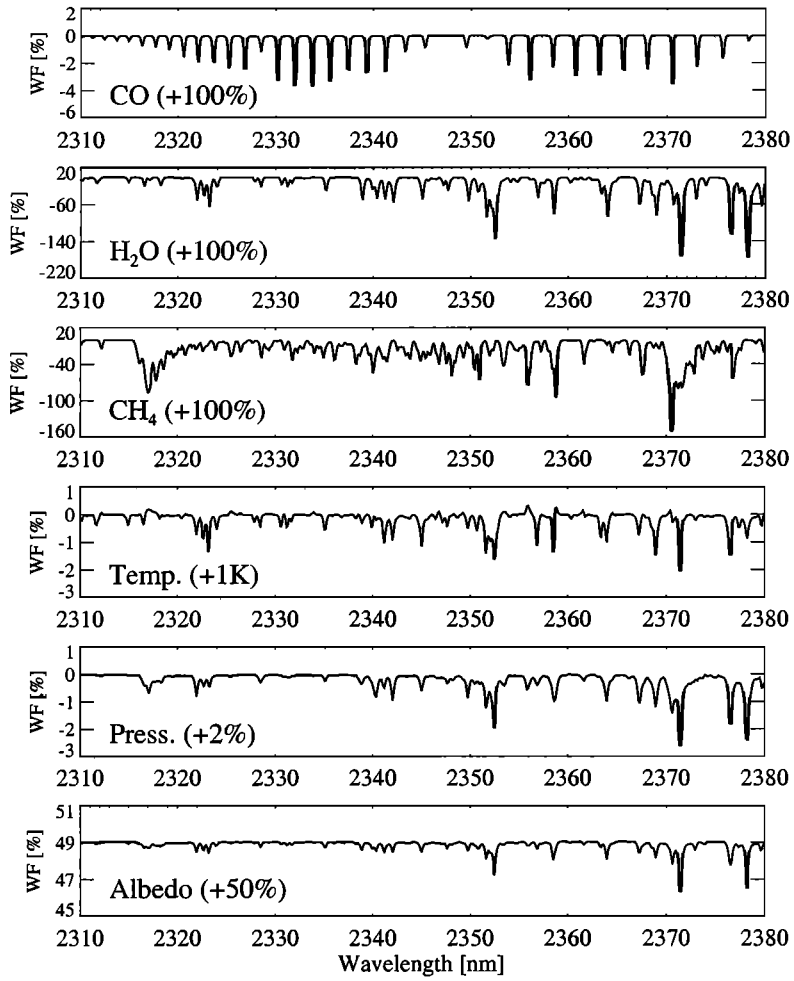

Figure 2. Dimensionless weighting functions (percentage intensity change assuming linearity) for altitude-independent perturbations of atmospheric and surface parameters. The first three panels show total column weighting functions corresponding to a trace gas concentration increase of +100% at each altitude (here WF [%] means $\partial \ln I/\partial V|_{V=\bar{V}} \times \bar{V} \times 100$, see (1)). The following panels show the weighting functions for temperature profile shift, pressure profile scaling, and albedo. The scenario is identical to Figure 1.

ized by maritime aerosol in the boundary layer. The visibility is that for a troposphere having background aerosol, that is, 23 km, and the relative humidity is 80%. Background aerosol has also been assumed for the stratosphere and the mesosphere. The solar zenith angle was 40° and the scan angle corresponds to exact nadir observation from space. The simulated measurements correspond to a scenario that significantly differs from the mean scenario to consider the typical variability of the atmosphere: the CO, H_2O and CH_4 number density profiles have been scaled by 1.4, 1.2, and 1.1, respectively. The pressure profile has been scaled with 1.02, corresponding to a +20 hPa change of the surface pressure, and the temperature profile has been shifted by 5 K. The albedo was 0.1 instead of 0.2. These parameters results in model radiances being roughly 2 times larger than the simulated measurements. Despite the large differences in atmospheric and surface parameters, the retrieved CO column agrees within 1% with the true column. Note that no iteration has been performed. The H_2O and CH_4 total columns agree to within 0.4% and 0.2%, respectively. The 5 K temperature profile shift was determined to within 0.1 K. These deviations are systematic errors resulting mainly from linearization errors. They could be further reduced by iteration. No noise has been added to the simulated measurements at this stage. Random errors due to noise will be discussed separately in section 5.

This excellent agreement of the fit parameters with the true atmospheric parameters indicates that the albedo and pressure weighting functions need not to be considered for accurate CO retrieval. This has also been confirmed by other test retrievals using different profiles, solar zenith angles, and albedos. Albedo effects on the radiance are well compensated by the polynomial even for large albedo differences between model and measurement scenarios (e.g., assuming 0.05 instead of 0.2). Although the albedo weighting function exhibits

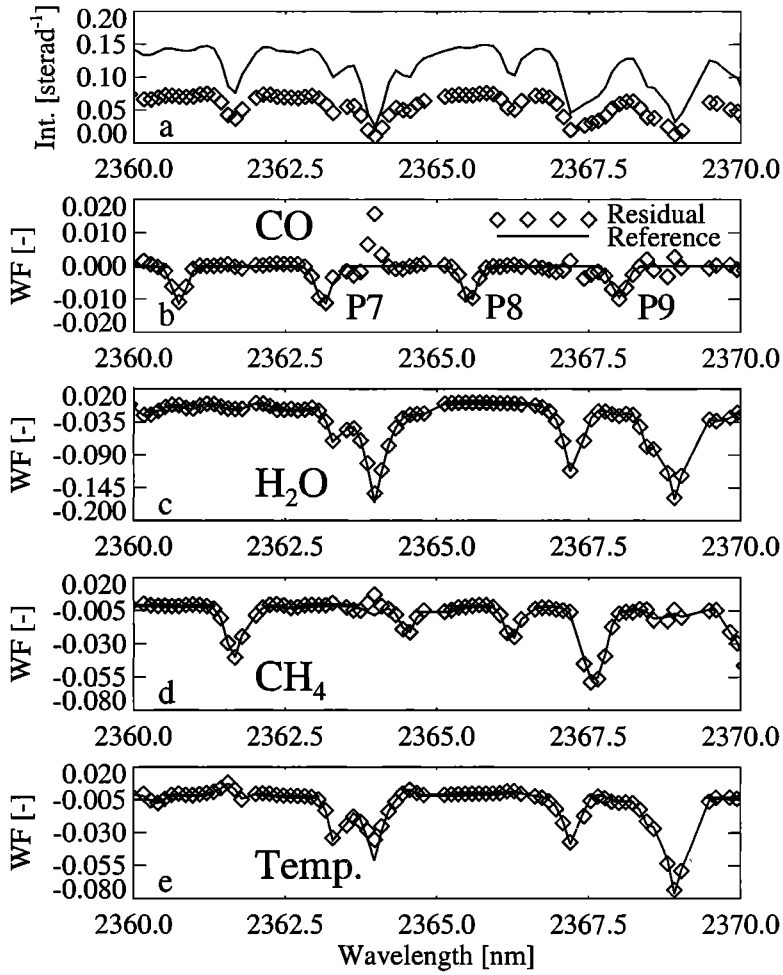

Figure 3. (a) Model intensity (solid line) and simulated measurement (squares). Each square corresponds to one detector pixel. (b) Solid line, CO total column weighting function (WF) scaled by CO column fit parameter ("CO Reference"), that is, $\partial \ln I^{\mathrm{mod}}/\partial V|_{V=\bar{V}} \times (\hat{V} - \bar{V})$. Squares, measurement minus linear least squares adjusted reference spectra except CO Reference, or, equivalently, CO Reference plus difference between measurement and adjusted model spectrum ("CO Residual"). As can be seen, the differential CO structures can be accurately identified in the measurement. All deviations from the CO Reference correspond to spectral regions containing strong H_2O or CH_4 absorption. (c-e) Similar as for Figure 3b but for H_2O, CH_4, and temperature. Fitting window is the entire CO band in channel 8 (2310-2380 nm). Only a small part is shown for clarity.

spectral structures (see last panel of Figure 2), the inclusion of the albedo weighting function in the linear fit generally does not result in a significant reduction of the CO total column error. Similar remarks hold for the aerosols as they also affect the radiance mainly in a broadband fashion. Even if aerosols are entirely neglected in the assumed model atmosphere, but are present in the observed atmosphere, the resulting CO column errors are still below $\sim 1\%$. A pressure (scaling) weighting function that may be included to compensate for pressure profile differences between model and measurement scenario is also not necessary (at least for typical surface pressure variations at constant ground altitude). As shown in Figure 2, the radiance changes less than 2% at SCIAMACHY resolution even for a large pressure change (2% increase at all altitudes resulting in a 20 hPa surface pressure change). In comparison, the temperature sensitivity of the radiance is about 2% per Kelvin.

The weighting functions for H_2O and CH_4 total columns and for a temperature shift, however, are important for accurate CO retrieval. Neglecting the temperature weighting function results in CO retrieval errors of up to 5-10%. If the temperature weighting function is included, the H_2O total column can be retrieved simultaneously with the CO column within a few percent. However, if the temperature weighting function is neglected, the H_2O total column may be wrong as much as 30%. The CH_4 total column error is generally less than 1% but may rise up to 3-4% if the temperature weighting function is neglected.

Using these trace gas and temperature fit parameters

along with the three fit parameters of the second-order polynomial suffices to accurately retrieve the CO column. The CO error was less than 3% for all scenarios investigated including large systematic deviations between model and measurement scenario of, for example, 100% differences in the CO and H_2O columns, 10% difference in the CH_4 column (note that the variability of CH_4 is rather low), 20 K difference in the temperature profile, 2% difference in the pressure profile, and large differences in albedo (e.g., 0.05 instead of 0.2) and aerosols (see above). Test retrievals have also been made for different profile shapes, that is, profile differences not restricted to altitude-independent scaling factors or offsets (shifts). Still the CO total column retrieval error was less than 3%. In this case, the retrieved value of the temperature shift parameter can be interpreted, to a good approximation, as the mean temperature difference between the true and the assumed model atmosphere in the lowermost 5 km.

An accuracy of better than 3% has also been established for the simultaneously derived CH_4 total column. The same holds for H_2O if the column differences between measurement and model are not too large (less than $\sim$ 50%). For large H_2O differences, the H_2O column error may exceed 5%. This may be explained by nonlinearities due to the strong water vapor absorption in combination with large column differences. This effect is much smaller for CO due to its weak absorption and for CH_4 due to its smaller variability. For H_2O retrieval one iteration would significantly improve the accuracy, or, alternatively, a fitting window where water vapor absorption is small (note that H_2O absorbs in nearly all channels of SCIAMACHY). In general, the temperature shift between the true and the model atmosphere can be retrieved to within better than 1-2 K. The error may be as large as 3 K if the temperatures deviate by 20 K. Similar results have also been obtained for N_2O retrieval in the spectral region 2265-2285 nm. Note that all errors reported in this study refer to a single linear regression, that is, no iteration has been performed.

The intensity and weighting function reference spectra depend on the solar zenith angle, on the line-of-sight scan angle, and on the relative azimuth angle between the instrument line of sight and the Sun direction. All these angles vary continuously over the orbit. In order to apply the algorithm to global total column retrieval, a look-up-table approach is presently envisaged to speed up the retrieval. This requires the selection of a relatively small set of reference spectra. A solution to this problem is to precalculate the reference spectra for exact nadir viewing geometry only, as a function of solar zenith angle. The solar zenith angle grid needs to be sufficiently fine to permit interpolation to arbitrary solar zenith angles (e.g., in steps of 2°-5° for the solar zenith angle range 15°-85°).

The scan and azimuth angle dependence of the reference spectra can be considered using a simple geometrical correction as demonstrated by Table 1, that is, no reference spectra are needed to account for different scan and azimuth angles. The table shows nadir scanning vertical column correction factors for different line-of-sight scan angles (φ) and for a constant solar zenith angle (ψ) of 70°. The values given for CO, H_2O, and CH_4 (columns 2-4) have been derived from simulated WFM-DOAS retrievals. The simulated radiance measurements have been calculated taking the scan angle dependence fully into account. The reference spectra, however, correspond to exact nadir viewing. The table shows the resulting percentage total column retrieval errors. These values can be used to correct the total column amounts determined with nadir-only reference spectra. As expected, the error increases with increasing line-of-sight scan angle and is zero for exact nadir observation. Without any correction, the retrieved columns would be overestimated by up to 4%. The last column shows the ratio of two geometrical path length determined for a plane-parallel atmosphere: the nominator corresponds to the path length for exact nadir viewing and the denominator to the path length corresponding to the actual scan angle, that is, $[(\cos(\varphi)^{-1} + \cos(\psi)^{-1}) \,/\, (1 + \cos(\psi)^{-1}) - 1] \times 100$. This simple approach closely reproduces the exact values given in columns 2-4.

Table 1. Nadir Scanning Vertical Column Correction Factors for Different Line-of-Sight Scan Angles and for a Constant Solar Zenith Angle of 70°.

Scan angle, deg.	CO, %	H_2O, %	CH_4, %	Geometric, %
30.0 E	3.7	3.2	3.7	3.9
22.5 E	2.2	2.2	2.1	2.1
15.0 E	1.0	1.2	1.0	0.9
07.5 E	0.3	0.5	0.3	0.2
00 0 N	0.0	0.0	0.0	0.0
07.5 W	0.1	0.0	0.1	0.2
15.0 W	0.8	0.5	0.9	0.9
22.5 W	1.9	1.7	1.9	2.1
30.0 W	3.8	3.4	3.8	3.9

Correction factors are last four columns. E refers to east of nadir, W refers to west of nadir (corresponding to different relative azimuth angles), and N refers to exact nadir observation (scan angle 0°). The last column contains the geometrical correction factor (see main text for details).

The retrieval errors due to linearization can be minimized by selecting for each solar zenith angle an appropriate atmosphere, for example, taking into account the much higher water vapor column in the tropics (corresponding to small solar zenith angles) compared to the polar regions (corresponding to large solar zenith angles). In order to better consider the seasonal variability of the atmosphere, interhemispheric differences, surface topography, and perhaps clouds, several atmospheres per solar zenith angle need to be defined. The

final size of a look-up-table for, for example, CO total column retrieval, has not yet been determined. It is expected that about 500 different sets of radiance and weighting function reference spectra will be sufficient to cover all conditions.

Cloud-contaminated ground pixels constitute an important problem for total column retrieval, particularly, as all the trace gases discussed here have a large fraction of their total column in the lower troposphere. As a significant number of the ground pixels will be at least partially contaminated by clouds, a scheme is required which retrieves accurate columns also for partially cloud covered pixels. As optically thin clouds behave similarly as the aerosols, the retrieval is expected to be insensitive to optically thin clouds due to the polynomial subtraction. One approach to solve the problem of significant cloud contamination is to use long-lived gases whose volume mixing ratios are well known and show much less variability than the trace gas of interest, such as O_2 or N_2O, to perform an air mass correction as described by *Noël et al.* [1999] for H_2O total column retrieval from GOME data by simultaneously fitting the O_2 absorption. This scheme also allows for a certain extent to correct for clouds. This important topic needs to be addressed specifically in a separate study.

The total column errors reported in this section are systematic retrieval errors (mainly linearization errors). They correspond to noise-free radiance measurements or to the mean systematic column difference with respect to the true column if noise is considered and the retrieval could be repeated many times. This, however, is not possible for SCIAMACHY, mainly due to the variability of the troposphere. Statistical measurement errors due to noise will be discussed in the following section.

5. Estimation of Total Column Retrieval Precisions

Noise on the radiance results in errors on the retrieved vertical columns. The uncertainty of a measured quantity due to noise is usually referred to as precision (1σ standard deviation). This section focuses on the estimation of vertical column retrieval precisions for several important trace gases from SCIAMACHY channels 7 and 8 nadir radiance and solar irradiance measurements for cloud-free conditions. In the following an integration time of 1 s is assumed for a single measurement corresponding to a ground pixel size of 30×240 km^2 (along track times across track) for the nominal (maximum) across-track line-of-sight scan angle range of $\pm$ 30°.

H_2O shows significant absorption in all SCIAMACHY channels except in the UV channels 1 and 2. CO and N_2O can only be retrieved from channel 8. CO_2 shows its strongest absorption in channel 7 but also absorbs significantly in channel 6 (1000-1750 nm). CH_4 strongly absorbs in channel 8 but also in channel 6. As this study focuses on channel 7 and 8 retrieval only, the precisions for H_2O, CO_2, and CH_4 reported here may be considered as upper limits (at least in theory, they can be improved by extending the spectral region used for retrieval).

The scatter of the intensity due to noise, characterized by a 1σ standard deviation, has been estimated using a numerical instrument model based on accurate instrument parameters, derived using detailed information from the detector manufacturers (EPITAXX Inc., Princeton, New Jersey, and SRON, Utrecht, Netherlands). The total noise is assumed to consist of several uncorrelated Gaussian noise terms. The most important terms are atmospheric photon shot noise, Johnson-Nyquist noise, that is, thermal noise of the detector diode resistance, dark current shot noise, shot noise due to thermal radiation emitted by the optical bench, and electronic readout noise. The channels 7 and 8 InGaAs detectors exhibit a significant detector pixel-to-pixel variability with respect to dark current and quantum efficiency which adds significantly to the noise. Individual detector pixels marked as not useful by the detector builders, for example, due to high dark current, have been masked out for this study and are termed dead pixels. The signal-to-noise ratios, that is, the standard deviation of the radiance divided by the mean radiance, are similar for channels 7 and 8 nadir measurements. They strongly depend on the atmospheric radiance level. Except for high radiance levels, corresponding to high albedo and low solar zenith angles, the signal-to-noise ratio is, to a good approximation, proportional to the atmospheric radiance. The mean relative radiance noise for channels 7 and 8, that is, the inverse of the signal-to-noise ratio averaged over a channel, is presented in the last columns of Tables 2 and 3 for a variety of conditions.

Channels 7 and 8 radiance spectra have been calculated for different atmospheres, solar zenith angles, and albedos to determine precision values representative for most of the conditions encountered by SCIAMACHY in orbit. The total column precision (i.e., the standard deviation of $\hat{V}$) is the square root of the corresponding diagonal element of the covariance matrix $\mathbf{C_x}$ (see (3)), multiplied by model column $\bar{V}$ (and correspondingly for the $\hat{b_j}$ total column fit parameters). Tables 2 and 3 summarize the main results using the entire channels 7 and 8 for retrieval, respectively. In addition to the trace gases listed in the tables, a temperature weighting function and a second-order polynomial has been included in matrix $\mathbf{C_x}$ in line with the WFM-DOAS results reported in the previous section. The precision does not depend significantly on the degree of the polynomial. As expected, the precision improves when the degree of the polynomial is reduced. Excluding the polynomial and the temperature weighting function from the fit, and modifying (1) such that the intensity is modeled rather than the logarithm of the intensity (note that the noise refers to the intensity and not to its logarithm) also does not change the precision much. The precision

Table 2. Trace Gas Total Column Precisions (1σ) for SCIAMACHY Channel 7 Nadir Measurements.

	Atmosphere	Solar Zenith Angle, deg.	Albedo	CO_2, %	H_2O, %	Mean Radiance Noise, %
1	USS	40	0.20	0.03	0.05	3.0
2	USSa	40	0.20	0.03	0.06	3.1
3	USSb	40	0.20	0.03	0.06	7.4
4	USS	60	0.03	0.22	0.40	11.9
5	USS	60	0.10	0.09	0.15	7.8
6	USS	60	0.20	0.05	0.08	5.9
7	USS	60	1.00	0.01	0.02	2.9
8	USS	85	0.20	0.55	0.63	54.3
9	USS	90	0.20	8.13	9.03	134.5

Total column precisions are in columns 5 and 6. USS refers to the U.S. Standard Atmosphere [*McClatchey et al.*, 1972]. USSa (USSb) is identical with USS, except that the CO_2 (H_2O) profile is scaled with 1.1 (2.0). The USS vertical columns are 7.1×10^{21} and 4.8×10^{22} molecules/cm^2 for CO_2 and H_2O, respectively. The mean radiance noise is the relative radiance noise (i.e., the 1σ standard deviation of the radiance divided by the mean radiance) averaged over all pixels of channel 7 (dead pixels are excluded).

improves by up to 30% for N_2O (e.g., 2.6% instead of 2%) and 50% for H_2O but is essentially unchanged for CO, CH_4, and CO_2.

For channel 7 measurements the total column precisions of CO_2 are better than 0.6% at solar zenith angles less than 90°. Best values are around 0.03%. Even for a minimum albedo of 0.03, corresponding to water- or snow-covered surfaces, the precision is as good as 0.2%. At solar zenith angles of 90° or larger the signal strongly decreases and the precision exceeds 8%. The channel 7 H_2O precision is approximately a factor of 2 worse compared to CO_2. For constant solar zenith angle the precision improves proportional to albedo (i.e., the inverse of the precision is proportional to albedo). For constant albedo the precision is approximately proportional to the cosine of the solar zenith angle. These values refer to retrievals using the entire channel 7. Restricting the retrieval to the 2025-2040 nm subrange of channel 7, the precisions are about 3 times worse, corresponding to a precision being proportional to the inverse of the square root of the number of detector pixels used for retrieval.

The channel 8 results are as follows: the total column precision of CH_4 is typically better than 0.5%, except for solar zenith angles larger than 85°. At 90° the precision may be as worse as 6%. The H_2O total column precisions are a factor of 4-5 worse compared to CH_4. For nearly all cases, the H_2O precision is better than 2%.

For CO, which is highly variable in the troposphere, the precision strongly depends on its amount, on the albedo, and on the solar zenith angle, and varies between about 2% and 17% for solar zenith angles less than 85°. For channel 8 measurements, albedos below 0.1 correspond to ground pixels dominated by snow-covered surfaces or by water. Minimum albedos are around 0.03-0.04. The albedo values referred to in this study are derived from a database of spectral albedos (at 100 nm spectral intervals in the NIR) for sand, soil, snow, and vegetation, covering the SCIAMACHY spectral region, compiled by Guzzi from various sources [see *Guzzi et al.*, 1998, and references therein] for the GOME and SCIAMACHY satellite projects. The albedo at 2300 nm is 0.49 for sand, 0.36 for soil, 0.2 for vegetation, and 0.045 for snow. The water albedo [*Guzzi et al.*, 1996] accounts for sea surface roughness and depends on wind speed and solar zenith angle. Assuming a wind speed of 10 m/s, the albedo is 0.03 at a solar zenith angle of 10°, 0.15 at a solar zenith angle of 60°, and about 0.32 for 85°. As can be seen, the precision improves nearly proportional with albedo. This holds for all four trace gases. For CO the precision improves nearly linearly with the CO vertical column. For N_2O the scenario dependence of the precision is similar to CO.

The channel 8 precisions discussed refer to a retrieval using the entire channel 8. For several reasons, for example, to speed up the retrieval or to avoid interference with other components, it might be attractive or even mandatory to restrict the retrieval to smaller spectral fitting windows. For CO and N_2O the precision is roughly proportional to the inverse of the square root of the number of moderate to strong lines located in a given fitting window. The channel 8 precisions reported here are in good agreement with values presented by *Schrijver et al.* [1998].

These results show that SCIAMACHY can provide important information on the global distribution and variability of key atmospheric constituents. Combining the nadir total column information with the nearly simultaneous limb observations of stratospheric and mesospheric profiles by SCIAMACHY, the tropospheric columns can be derived [*Bovensmann et al.*, 1999].

6. Potential Application of SCIAMACHY Measurements for the Study of Greenhouse Constituents and Their Emission Fluxes

The most important greenhouse gases in the troposphere are H_2O, CO_2, CH_4, N_2O, and the CFCs (chlorofluorocarbon compounds). Similarly, clouds, aerosols and the Earth's surface spectral reflectance play important roles in global climate change.

CO_2, CH_4, and N_2O, whose total column amounts are all retrieved from SCIAMACHY observations, are specifically listed in Annex A of the protocol of the Third Conference of Parties to the U.N. Framework Convention on Climate change held in Japan in December 1997. The international agreement reached at

Table 3. Trace Gas Total Column Precisions (1σ) for SCIAMACHY Channel 8 Nadir Measurements.

	Atmosphere	Solar Zenith Angle, deg.	Albedo	CO, %	CH_4, %	H_2O, %	N_2O, %	Mean Radiance Noise, %
1	TRO	25	0.20	2.7	0.1	0.2	1.9	1.9
2	USSc	40	0.20	5.1	0.1	0.4	2.0	0.6
3	USS	40	0.20	2.6	0.1	0.4	2.0	0.6
4	USSd	40	0.20	2.1	0.1	0.4	2.0	0.6
5	MLS	50	0.20	3.0	0.1	0.3	3.3	1.8
7	USS	60	0.03	16.8	0.8	2.7	12.3	5.5
8	USS	60	0.10	6.0	0.3	1.0	4.5	2.1
9	USS	60	0.20	3.2	0.1	0.5	2.4	1.1
10	USS	60	0.30	2.2	0.1	0.3	1.7	0.8
11	USS	60	1.00	0.7	0.1	0.1	0.6	0.3
12	USS	80	0.20	5.5	0.4	1.3	3.9	8.2
13	SAS	80	0.20	5.7	0.4	1.2	4.3	11.8
14	USS	85	0.20	8.5	0.7	2.5	5.8	24.2
15	USS	90	0.20	60.5	6.2	25.0	34.8	204.0

Total column precisions are in columns 5-8. The atmospheric identifiers refer to the following atmospheres [*McClatchey et al.*, 1972]: TRO, tropical; USS, U.S. Standard Atmosphere; USSc, as USS but CO profile scaled with 0.5; USSd, as USS but CO profile scaled with 1.3; MLS, midlatitude summer; SAS, subarctic summer. The USS atmosphere vertical columns in Dobson units ($= 2.7\times10^{16}$ molecules/cm^2) are CO, 89; CH_4, 1322; H_2O, 1.8×10^6; N_2O, 246. See caption of Table 2 for the definition of mean radiance noise.

this meeting is known as the Kyoto Protocol. The Kyoto Protocol assigns each country an entitlement to emit not more than a fixed quantity of greenhouse gases during a 5-year commitment period commencing in 2008. Within the European Union, which in total committed itself to an 8% greenhouse gas emission reduction with respect to 1990 levels, the regional emission trends might differ significantly. For example, France and Finland have proposed no reduction, whereas Germany has proposed a 21% reduction and Portugal and Greece are expected to increase their emissions by about 25% with respect to the 1990 levels (H. Meyrahn, private communication, 1999).

The origin of the increase of CO_2 is assumed to be dominated by fossil fuel combustion. In comparison, the origin of the increase in CH_4 and in N_2O is not well established [*Intergovernmental Panel on Climate Change (IPCC)*, 1995]. The CH_4 increase slowed in the early 1990s but has increased since about 1993, the reasons being still a matter of scientific discussion [*Rudolph*, 1994; *Worthy et al.*, 1998].

From the above there is a clear need to monitor the anthropogenic emissions of greenhouse gases from continents or countries to show compliance with the agreed aims of the Kyoto Protocol and to establish the processes responsible for the changes in the abundance of other greenhouse gases. It is therefore of significance to investigate the role of global measurements of these species by SCIAMACHY or SCIAMACHY-like measurements.

From Tables 2 and 3 it can be concluded that the detection limits for total column changes of the greenhouse gases CO_2, CH_4, and N_2O are of the order of 0.5%, 1%, and 10%, respectively. This corresponds to a single measurement detection limit of 4×10^{19} molecules/cm^2 for CO_2, 4×10^{17} molecules/cm^2 for CH_4, and 7×10^{17} molecules/cm^2 for N_2O (for the U.S. Standard Atmosphere).

In this section the potential to estimate regional greenhouse gas emission fluxes from SCIAMACHY total column measurements is investigated. Inferring this information from real SCIAMACHY measurements is a complex task that has to consider the dynamics and chemistry of the Earth's atmosphere along with the distribution of emission sources and the actual scan pattern. In this study an idealized situation with respect to the meteorological condition, the distribution of emission sources, and the scan pattern is assumed to derive lower limits of the emission flux errors taking into account the total column precisions reported in the previous section. The regional emission flux and its error is simply derived from the difference of total columns measured downwind and upwind of a given area, taking into account the wind speed and the horizontal dimension. Air parcels in the boundary layer are assumed to accumulate the chemically relatively inert greenhouse

gases emitted by various sources on their passage across a given area. For a typical horizontal scale of 500 km and wind speeds between 1 and 10 m/s the accumulation time varies between 0.5×10^5 and 5×10^5 s (0.6-6 days).

The estimated energy-related CO_2 emissions of Germany, the United Kingdom, and Japan are 1030, 600, and 1060 Tg/yr, respectively [see *Enquete Commission*, 1992, and references therein]. This corresponds to an emission flux of roughly 10^{14} molecules/cm^2/s (respective areas: 350, 250, and 370 $\times 10^3$ km^2), or, to a total column increase of 0.5-5 $\times 10^{19}$ molecules/cm^2 for the range of accumulation times given above. This corresponds to a total column gradient of 0.07-0.7% per 500 km. Assuming that the accumulation results in a constant volume mixing ratio (VMR) increase restricted to a 1 km boundary layer, this is equivalent to a VMR change by 2-20 ppm per 500 km. A comparison with the 0.5% or 4×10^{19} molecules/cm^2 CO_2 detection limit shows that for the specified conditions the total column increase corresponding to the 500 km horizontal path is, depending on wind speed, close to or below the detection limit for a single CO_2 total column difference measurement.

This can be improved by averaging. For the following analysis, it is assumed that the detection limit improves proportional with the square root of the number of total column measurements added. Strictly speaking, this requires identical (but noisy) measurements to be repeated many times. This is in line with the idealized steady state situation analyzed here but may not be justified for real SCIAMACHY measurements, for example, due to emission source variability and due to the variability of the atmosphere (despite of the low variability of the trace gases investigated here, i.e., CO_2, CH_4, and N_2O). In this paragraph, it shall be indicated how this averaging may essentially be achieved using the real SCIAMACHY data. A detailed discussion on the best approach how to use the real SCIAMACHY measurements to derive emission fluxes is, however, out of the scope of the present study. Furthermore, this requires real data to be analyzed. In order to estimate, for a given time period and a given region, the mean emission flux and the emission trend, the Earth's surface could be divided into regions of, for example, 500×500 km^2. For each region a representative mean CO_2 column can be determined and possibly also the linear trend in the CO_2 column, by fitting a straight line to a time series of single pixel total column measurements using, for example, several years of SCIAMACHY data. This may require a certain amount of preprocessing, for example, the subtraction of seasonal effects. The desired regionally averaged emission flux and its trend (both valid for the analyzed time period) may then be determined by solving the following problem: Given a three-dimensional (3-D) transport/chemistry model of the atmosphere (e.g., using analyzed meteorological fields) with adjustable regional emission source strength, which set of regional emission fluxes and trends (two numbers for each region) reproduces the regional mean total column and total column trend measurements (two numbers plus errors for each region) within measurement error?

Monthly averages for 500×500 km^2 regions may be generated from up to 500 individual SCIAMACHY measurements. Assuming that only 50% of these data are sufficiently cloud-free, results in 250 useful single measurements per month. Even using 50% of all pixels may require a correction algorithm that enables accurate total columns to be retrieved also for ground pixels partially covered by clouds (note the discussion related to this issue at the end of section 4). Averaging 250 measured column differences improves the detection limit by a factor of about 16 in comparison with a single measurement resulting in 0.25×10^{19} molecules/cm^2. For these conditions the CO_2 emission signal is a factor of 2-20 larger than the detection limit, corresponding to CO_2 emission measurement errors between 5% (wind speed 1 m/s) and 50% (10 m/s). With respect to the 5-year nominal lifetime of SCIAMACHY these errors can, at least for the simplified steady state situation discussed here, be further reduced by up to a factor of 7 ($\approx \sqrt{12 \times 5}$) resulting in regional emission flux errors of approximately 1-7% using 5 years of SCIAMACHY data.

The methane emissions of Germany and the United Kingdom due to animal farming (enteric fermentation of ruminant animals) are estimated to be 1200 and 900 Gg/yr, respectively [see *Enquete Commission*, 1992, and references therein]. The corresponding column increase, assuming the same conditions as for CO_2, is 1-10 $\times 10^{16}$ molecules/cm^2 or 0.07-0.7%. This corresponds to a VMR increase of 10-100 ppb in a 1 km boundary layer. Using 500×500 km^2 monthly averages or, equivalently, averaging 250 measured column differences, results in emission flux measurement errors between approximately 10% (wind speed 1 m/s) and 100% (10 m/s). Using 5 years of SCIAMACHY data, these errors may be reduced to 2%-14%.

The N_2O total column precision of 7×10^{17} molecules per cm^2 for a single measurement corresponds to a VMR increase in a 1 km boundary layer of 290 ppb. The background tropospheric N_2O VMR is 311 ppb (1997) and increases by about 0.2% per year [*Nakazawa et al.*, 1997]. N_2O has a long tropospheric lifetime and is well mixed. The spatial and temporal variability is generally less than a few ppb. Averaging 250 column differences for an area of 500×500 km^2 reduces the detection limit to about 18 ppb. This, however, in general, seems not to be sufficient to measure regional N_2O emissions with acceptable accuracy.

The emission flux errors estimated in this section have to be interpreted as lower limits as only noise has been accurately considered, that is, the final errors of the real

measurements are expected to be larger. In practice, the most accurate assessment of emission fluxes from real SCIAMACHY measurements may be achieved using two-dimensional emission source strength distributions and 3-D transport and chemistry models of the atmosphere.

7. Conclusions

The first detailed investigation concerning atmospheric trace gas retrieval from space using SCIAMACHY near-infrared nadir radiance measurements around 2 μm has been presented. A modified DOAS algorithm (WFM-DOAS) has been introduced to be used for the global determination of trace gas total column amounts. It has been shown that the retrieval problem is sufficiently linear to apply a fast linear least squares algorithm based on a relatively small look-up-table of precalculated radiance and weighting function reference spectra. The algorithm is quite insensitive to uncertainties in interfering atmospheric or surface parameters such as pressure, temperature, interfering trace gases, aerosols, and albedo. In addition, the algorithm is insensitive with respect to broadband residual calibration errors.

The total column retrieval precisions of the trace gases CH_4, CO, CO_2, H_2O, and N_2O for SCIAMACHY channels 7 and 8 nadir measurements have been estimated for a variety of conditions. They are, in general, better than 1% for H_2O, CO_2, and CH_4 and better than 10% for N_2O and CO.

The spectral regions around 2.2 and 2.3 μm, covered by channel 8 and investigated in this study, are also covered by the MOPITT gas correlation instrument launched in December 1999 on board EOS Terra. The estimated retrieval precisions of the MOPITT CO and CH_4 total column measurements are similar as the values established here for SCIAMACHY, that is, about 10% for CO and 1% for CH_4 [*Pan et al.*, 1998].

The potential of SCIAMACHY to measure regional CO_2 and CH_4 emission fluxes has been investigated assuming simplified conditions with respect to atmospheric dynamics, scan pattern, and source variability. The estimated (best case) errors indicate that the total column measurements of SCIAMACHY in combination with 3-D source/sink transport/chemistry models of the atmosphere might contribute to the assessment of Kyoto Protocol compliance. This, however, needs further studies based on real SCIAMACHY measurements.

The important problem of trace gas total column retrieval using partially cloud-contaminated ground pixels also needs to be investigated in a separate study especially to maximize the information obtained about long-lived tropospheric species such as CO_2, CH_4, and N_2O, which have small variability.

Acknowledgments. This work has been funded in parts by the German Ministry for Science and Education BMBF (grant 07 UFE 12/8), represented by the GSF, Munich, Germany, and by the State and the University of Bremen. We thank our colleagues S. Noël, A. Richter, and M. Weber for helpful discussions, and Dr. H. Meyrahn, Rheinbraun AG, Cologne, Germany, for providing information related to the Kyoto Protocol.

References

Barkstrom, B. R., A finite differencing method of solving anisotropic scattering problems, *J. Quant. Spectrosc. Radiat. Transfer, 16,* 725-739, 1976.

Bovensmann, H., J. P. Burrows, M. Buchwitz, J. Frerick, S. Noël, V. V. Rozanov, K. V. Chance, and A. P. H. Goede, SCIAMACHY: Mission objectives and measurement modes, *J. Atmos. Sci., 56,* 127-150, 1999.

Buchwitz, M., V. V. Rozanov, and J. P. Burrows, Development of a correlated-k distribution band model scheme for the radiative transfer program GOMETRAN/SCIATRAN for retrieval of atmospheric constituents from SCIAMACHY/ENVISAT-1 data, edited by J. E. Russell, in *Proc. SPIE Int. Soc. Opt. Eng., 3495,* 171-186, 1998.

Buchwitz, M., V. V. Rozanov, and J. P. Burrows, A correlated-k distribution scheme for the radiative transfer model GOMETRAN/SCIATRAN: Accuracy, speed, and applications, in *Proceedings ESAMS'99 - European Symposium on Atmospheric Measurements from Space,* pp. 765-770, ESA Earth Sci. Div., Eur. Space Res. and Technol. Cent., Noordwijk, Netherlands, 1999.

Buchwitz, M., V. V. Rozanov, and J. P. Burrows, A correlated-k distribution scheme for overlapping gases suitable for retrieval of atmospheric constituents from moderate resolution radiance measurements in the visible/near-infrared spectral region, *J. Geophys. Res.,* in press, 2000.

Burrows, J. P., E. Hölzle, A. P. H. Goede, H. Visser, and W. Fricke, SCIAMACHY - Scanning Imaging Absorption Spectrometer for Atmospheric Chartography, *Acta Astronaut., 35,* 445-451, 1995.

Burrows, J. P., et al., The Global Ozone Monitoring Experiment (GOME): Mission concept and first scientific results, *J. Atmos. Sci., 56,* 151-175, 1999.

Crutzen, P. J., M. G. Lawrence, and U. Pöschl, On the background photochemistry of tropospheric ozone, *Tellus, 51,* 123-146, 1999.

Daniel, J. S., and S. Solomon, On the climate forcing of carbon monoxide, *J. Geophys. Res., 103,* 13,249-13,260, 1998.

Diebel, D., R. de Beek, J. P. Burrows, B. Kerridge, R. Munro, U. Platt, L. Marquard, and K. Muirhead, Trace gas study: Detailed analysis of the retrieval algorithms selected for the level 1-2 processing of GOME data, *Tech. Rep., Eur. Space Agency (ESA),* pp. 5-150 (section 5), 1995.

Edwards, D. P., C. M. Halvorson, and J. C. Gille, Radiative transfer modeling for the EOS Terra satellite Measurement of Pollution in the Troposphere (MOPITT) instrument, *J. Geophys. Res., 104,* 16,755-16,775, 1999.

Eisinger, M., and J. P. Burrows, Tropospheric sulfur dioxide observed by the ERS-2 GOME instrument, *Geophys. Res. Lett., 25,* 4177-4180, 1998.

Enquete Commission, "Protecting the Earth's Atmosphere" of the 12th German Bundestag, *Climate Change - A Threat to Global Development,* Economia Verlag, Bonn, Germany, 1992.

Guzzi, R., J. P. Burrows, V. V. Rozanov, K. V. Chance, M. Cervino, T. Kurosu, and P. Watts, A study of cloud detection, ESA Contract Study 10997/94/NL/CN Final Report, Eur. Space Agency, Eur. Space Res. and Technol. Cent., Noordwijk, Netherlands, 1996.

Guzzi, R., J. P. Burrows, M. Cervino, and T. Kurosu, GOME Cloud and Aerosol Data Products Algorithm De-

velopment (CADAPA), ESA Contract Study 11572/95/NL/CN Final Report, Eur. Space Agency, Eur. Space Res. and Technol. Cent., Noordwijk, Netherlands, 1998.

Hoogen, R., Aerosol parameterization in GOMETRAN++, tech. report, 31 pp., Institut für Fernerkundung/Umweltphysik, Univ. of Bremen, Bremen, Germany, 1995.

Hoogen, R., V. V. Rozanov, and J. P. Burrows, Ozone profiles from GOME satellite data: Algorithm description and first validation, *J. Geophys. Res., 104,* 8263-8280, 1999.

Intergovernmental Panel on Climate Change (IPCC), *Climate Change 1995: The science of climate change*, edited by J. T. Houghton et al., Cambridge Univ. Press, New York, 1995.

Kauss, J., Aerosol Parametrisierung für Strahlungstransport-Simulationen im ultravioletten bis nahinfraroten Spektralbereich, Diploma thesis, 91 pp., Inst. für Fernerkundung/Umweltphysik, Univ. of Bremen, Bremen, Germany, 1998.

Kneizys, F. X., et al., The MODTRAN 2/3 report and LOWTRAN 7 model, edited by L. W. Abreu and G. P. Anderson, contract F19628-91-C-0132 with Ontar Corp., 261 pp., Phillips Lab., Geophys. Dir., Hanscom AFB, Mass., 1996.

Kurosu, T., V. V. Rozanov, and J. P. Burrows, Parameterization schemes for terrestrial water clouds in the radiative transfer model GOMETRAN, *J. Geophys. Res., 102,* 21,809-21,823, 1997.

Kurosu, T., K. V. Chance, and R. J. D. Spurr, Cloud retrieval algorithm for the European Space Agency's Global Ozone Monitoring Experiment, in *Satellite Remote Sensing of Clouds and the Atmosphere III*, edited by J. E. Russell, *Proc. SPIE Int. Soc. Opt. Eng. 3495,* 17-26, 1998.

McClatchey, R. A., R. W. Fenn, J. E. Selby, F. E. Volz, and J. S. Garing, Optical properties of the atmosphere, *3rd. edn. AFCRL-72-0497, Environ. Res. Pap. 411,* 108 pp., Airforce Cambridge Res. Lab., Bedford, Mass., 1972.

Nakazawa, T., S. Sugawara, G. Inoue, T. Machida, S. Makshyutov, and H. Mukai, Aircraft measurements of the concentrations of CO_2, CH_4, N_2O, and CO and the carbon and oxygen isotopic ratios of CO_2 in the troposphere over Russia, *J. Geophys. Res., 102,* 3843-3859, 1997.

Noël, S., M. Buchwitz, H. Bovensmann, R. Hoogen, and J. P. Burrows, Atmospheric water vapor amounts retrieved from GOME satellite data, *Geophys. Res. Lett., 26,* 1841-1844, 1999.

Pan, L., J. C. Gille, D. P. Edwards, P. L. Bailey, and C. D. Rodgers, Retrieval of tropospheric carbon monoxide for the MOPITT experiment, *J. Geophys. Res., 103,* 32,277-32,290, 1998.

Press, W. H., S. A. Teukolsky, W. T. Vetterling, and B. P. Flannery, *Numerical Recipes in FORTRAN: The Art of Scientific Computing*, 963 pp., Cambridge Univ. Press, New York, 1992.

Reichle, H. G., V. S. Connors, J. A. Holland, R. T. Sherrill, H. A. Wallio, J. C. Casas, E. P. Condon, B. B. Gormsen, and W. Seiler, The distribution of middle tropospheric carbon monoxide during early October 1984, *J. Geophys. Res., 95,* 9845-9856, 1990.

Richter, A., Absorptionsspektroskopische Messungen stratosphärischer Spurengase über Bremen, 55°N, Ph. D. thesis, Inst. für Umweltphysik, Univ. of Bremen, Bremen, Germany, 1997.

Richter, A., F. Wittrock, M. Eisinger, and J. P. Burrows, GOME observations of tropospheric BrO in the northern hemispheric spring and summer 1997, *Geophys. Res. Lett., 25,* 2683-2686, 1998.

Rodgers, C. D., Retrieval of atmospheric temperature and composition from remote measurements of thermal radiation, *Rev. Geophys., 14,* 609-624, 1976.

Rothman L. S., et al., The HITRAN molecular spectroscopic database and HAWKS (HITRAN atmospheric workstation): 1996 Edition, *J. Quant. Spectrosc. Radiat. Transfer, 60,* 665-710, 1998.

Rozanov, V. V., D. Diebel, R. J. D. Spurr, and J. P. Burrows, GOMETRAN: A radiative transfer model for the satellite project GOME: The plane-parallel version, *J. Geophys. Res., 102,* 16,683-16,695, 1997.

Rozanov, V. V., T. Kurosu, and J. P. Burrows, Retrieval of atmospheric constituents in the UV-visible: A new quasi-analytical approach for the calculation of weighting functions, *J. Quant. Spectrosc. Radiat. Transfer, 60,* 277-299, 1998.

Rudolph, J., Anomalous methane, *Nature, 368,* 19-20, 1994.

Schrijver, H., A. P. H. Goede, M. R. Dobber, and M. Buchwitz, Retrieval of carbon monoxide, methane and nitrous oxide from SCIAMACHY measurements, *Proc. SPIE Int. Soc. Opt. Eng.*, in *Optical Remote Sensing of the Atmosphere and Clouds*, edited by J. Wang, B. Wu, T. Ogawa, and Z. Guan, *3501,* 215-224, 1998.

Shettle, E. P., and R. W. Fenn, Models of the aerosols of the lower atmosphere and the effects of humidity variations on their optical properties, *Tech. Rep., AFGL-TR-79-0214, ADA 085951,* Air Force Geophys. Lab., Bedford, Mass., 1979.

Solomon, S., Stratospheric ozone depletion: A review of concepts and history, *Rev. Geophys., 37,* 275-316, 1999.

Stammes, P., Errors in UV reflectivity and albedo calculations due to neglecting polarization, *Proc. SPIE Int. Soc. Opt. Eng. 2311,* 227-235, 1994.

Vountas, M., V. V. Rozanov, and J. P. Burrows, Ring effect: Impact of rotational Raman scattering on radiative transfer in Earth's atmosphere, *J. Quant. Spectrosc. Radiat. Transfer, 60,* 943-961, 1998.

Worthy, D. E. J., I. Levin, N. B. A. Trivett, A. J. Kuhlmann, J. F. Hopper, and M. K. Ernst, Seven years of continuous methane observations at a remote boreal site in Ontario, Canada, *J. Geophys. Res., 103,* 15,995-16,007, 1998.

M. Buchwitz, J. P. Burrows, and V. V. Rozanov, Institut für Fernerkundung, Universität Bremen, Postfach 330440, 28334 Bremen, Germany.
(Michael.Buchwitz@ife.physik.uni-bremen.de;
John.Burrows@ife.physik.uni-bremen.de;
Vladimir.Rozanov@ife.physik.uni-bremen.de)

(Received September 30, 1999; revised January 18, 2000; accepted March 13, 2000.)